IJE TRANSACTIONS C: Aspects Vol. 27, No. 6, (June 2014) 839-854

International Journal of Engineering

Journal Homepage: www.ije.ir

Adsorption of Malachite Green from Aqueous Solution using Activated Ntezi Clay: Optimization, Isotherm and Kinetic Studies

R. O. AJEMBA

Department of Chemical Engineering, Nnamdi Azikiwe University, Awka, Anambra, Nigeria

P A P E R I N F O

Paper history:
Received 10 August 2013
Accepted in revised form 12 December 2013

Keywords:
Adsorption
Equilibrium
Kinetics
Isotherm
Optimization
Malachite green
Clay

A B S T R A C T

The adsorption of malachite green from aqueous solution using a local low cost adsorbent, acid activated Ntezi clay, was investigated. The low cost adsorbent was activated with different concentrations of sulphuric acid and the physicochemical properties of the adsorbent were determined. The structural properties were also analyzed using XRF and XRD. The adsorption process was studied as a function of different process parameters such as temperature, adsorbent dosage, contact time, particle size and stirring speed. These process parameters were optimized using response surface methodology (RSM). The significance of the different process parameters and their combined effect on the adsorption efficiency has been established through a full factorial central composite design. The equilibrium modeling was analyzed using Langmuir, Freundlich, Dubini-Radushkevich and Temkin isotherm equations. The experimental results follow the Langmuir adsorption isotherm. Adsorption kinetics follows the pseudo-second order equation with intra-particle diffusion as the rate-determining step. This investigation has shown that local mineral clay can be modified and used as a good adsorbent for removal of impurities from contaminated water.

doi: *10.5829/idosi.ije.2014.27.06c.03*

1. INTRODUCTION

Dyes are increasingly being produced and used as colourants in many industries, such as textile, pharmaceutics, printing, pulp and paper, plastics, iron-steel, etc. Dyes are toxic and carcinogenic compounds; they are recalcitrant and thus stable in the receiving environment, posing a serious threat to human and environmental health.

A basic, cationic dye, malachite green (MG), tri-phenyl methane dye has been widely used for the dyeing of leather, wool, jute and silk and in distilleries. It also functions as fungicide and antiseptic in aquaculture industry [1]. Malachite green has properties that make it difficult to remove from aqueous solutions and also toxic to major microorganisms. Malachite green is environmentally persistent and acutely toxic to a wide range of aquatic and terrestrial animals. Several studies have shown MG to be highly lethal to fresh water fish, in both acute and chronic exposures. It causes serious public health hazards and also poses potential environmental problems. Both clinical and experimental observations reported so far reveal that, MG is a multi-organ toxin. It decreases food intake, growth and fertility rates; causes damage to liver, spleen, kidney and heart; inflicts lesions on skin, eyes, lungs and bones and produces teratogenic effects.

To protect the ecosystem and environment from contamination, the dye-stained wastewater from the industries must be treated before releasing into the environment. Owning to their resistance to photo-degradation, biodegradation and oxidizing agents [2] , biological processes are not useful or efficient methods for the removal of dyes from effluent. Most of the conventional methods of wastewater treatment such as coagulation and flocculation, sedimentation and floatation, membrane filtration, disinfection are either expensive or ineffective. These technologies mostly transform pollutants from one phase to another and do not completely eliminate them [3]. These inadequacies associated with the conventional methods have compelled Scientists and Researchers to search for novel effective and economical methods of dye removal.

*Corresponding Author Email: ginaajemba@rocketmail.com (R. O. AJEMBA)

Adsorption has been recognized as a potential technology for the removal of dyes from wastewater. In comparison to other physical, chemical and biological methods available for the treatment of textile industry effluent, adsorption is the most preferred technique due to simple and flexible design and easy operation [4]. The common adsorbent, activated carbon, has good capacity of removing pollutants, but its main disadvantages are high cost of treatment and difficult regeneration which increases the cost of wastewater treatment [5, 6]. Therefore, there is a necessity in finding low cost, locally available materials, renewable materials as sorbent for dye removal.

Various low-cost adsorbents that have been successfully implemented for the adsorption of dyes from wastewater are natural and modified clays [4], spent brewery grain [7, 8] modified agricultural by-products [9], industrial wastes [10], coir pith [11]. Natural clays are acquiring prominence as low-cost adsorbents over the last few decades due to their local and abundant availability and the capability to undergo modification to enhance the surface area, adsorption capacity and range of applicability [12-14]. The adsorption capacity of natural clay is hampered by its small surface area and this has led to the need for research and development in the field of modification of clay surfaces to enhance their adsorptive properties [15-18]. The removal of MG and fast green dyes were studied on montmorillonite clay adsorbent under optimized conditions. From the percentage removal data, it was reported that, fast green-montmorillonite clay system and MG-montmorillonite clay system shows about 97 and 95% adsorption tendency with 33.45 and 1.42 mg/g adsorption capacity, respectively. The potential use of a low cost inorganic powder (Persian Kaolin) for removal of basic yellow 28 (BY28), methylene blue and MG from aqueous solution has been reported. The values of the adsorption capacity of kaolin towards the cationic dyes ranged from 16 mg/g to 52 mg/g, being probably dependent on the geometry of the dye molecules [19]. The aim of this work is to investigate the adsorption efficiency of acid modified bentonite from Ntezi in removing chemical contaminant, malachite green, from aqueous solution and also investigate the kinetics and mechanism involved in dye adsorption on the acid activated bentonite. Furthermore, thermodynamic parameters were also determined. Response surface methodology has been applied to optimize and evaluate interactive effects of adsorption independent variables.

2. EXPERIMENTAL METHODS

2. 1. Preparation of the Bentonite Sorbent The bentonite used in this study was mined from Ntezi (N: 8° 32' 05"; E: 8° 55' 05"; A: 126m) in Ebonyi state, Nigeria. The mined clay was sun-dried for 48 hours and grinded to smaller particles using mortar and pestle. The ground samples were sieved to remove impurities and oven dried at 105^0C. The samples were then reacted with known concentrations (0.5mol L^{-1}, 1.0mol L^{-1}, 1.5mol L^{-1}, and 2.00mol L^{-1}) of sulphuric acid in a 250 cm^3 flask placed in a regulated water bath. The flask was heated while continuously being stirred. At the completion of the heating time, the slurry was removed from the bath and allowed to cool. After the cooling, the slurry was removed, filtered via a Buchner funnel and the clay residue was washed several times with distilled water, followed by filtration until the filtrate was neutral to pH indicator paper. The prepared wet sample was then dried in an oven at 120 ^{0}C over night. The lumps of the prepared clay samples were crushed and sieved into the required particle sizes and stored for use in the adsorption studies. The activated clay sample was then analyzed using XRF and XRD.

2. 2. Adsorption Studies The adsorption studies of the malachite green onto activated Ntezi bentonite (NB1.5) was studied according to the central composite full factorial design. A measured quantity of the activated bentonite was added to 100 ml solution of the prepared dye solution in 250 ml Erlenmeyer flasks. The mixture was agitated in an incubated shaker at a pre-determined temperature and speed for the desired time. At the completion of the reaction period, the supernatant was separated by centrifugation at 3000 rpm for 15 min, the residual concentration in the supernatant was determined. The dye concentration in the raw and treated sample was determined by UV-Vis spectrophotometer (model WFJ 525). The analyses were carried out at a wavelength of 619 nm. The response, removal efficiency of malachite green by the activated bentonite, was calculated as:

$$Y(\%) = 100\frac{c_0 - c_i}{c_0} \quad (1)$$

where c_0 and c_i are the initial and final concentration of the dye solution. The effect of initial dye concentration and pH were studied at the optimized conditions of the process variables, temperature, contact time, adsorbent dosage, particle size, and stirring speed. The amount of equilibrium adsorption, q_e (mg/g), was calculated by:

$$q_e = \frac{V(c_0 - c_e)}{M} \quad (2)$$

where c_0 and c_e (mg/l) are the liquid-phase concentrations of dye at initial and equilibrium, respectively, V(L) is the volume of the solution and M (g) is the mass of dry prepared sorbent used.

2. 3. Determination of pH Point of Zero Charge (pH_{PZC}) The pH point of zero surface charge characteristics of NB1.5 was determined using the solid addition method. 40 ml of 0.1 M NaCl solution were

transferred to a series of 250 ml stoppered conical flasks. The pH_i values of the solutions were adjusted between 2 and 11 by adding either 0.1 M HCl or NaOH and were measured using a Consort C931 pH meter (Belgium). The total volume of the solution in each flask was adjusted to exactly 50 cm^3 by adding NaCl solution of the same strength. The pH_i of the solution was then accurately noted. 0.5 g of NB1.5 was added to each flask, and the flask was securely capped immediately. The suspensions were then kept shaking for 24 h and allowed to equilibrate for 0.5 h. The final pH values of the supernatant liquids were noted. The difference between the initial and final pH (pH_f) values (ΔpH) was plotted against the pH_i. The point of intersection of the resulting curve with the pH_i axis, i.e. at $\Delta pH = 0$, gave the pH_{PZC}.

2. 4. Isothermal and Kinetic Studies The effect of contact time on the adsorption of malachite green has been analyzed by evaluating the kinetic data by pseudo-first order, pseudo-second order, Elovich, Bangham, and Intra-particle kinetic models. The adsorption isotherms have been evaluated to analyze the equilibrium data. Adsorption isotherm is the equilibrium relationship between the concentration in the liquid phase and the concentration in the adsorbent phase in the adsorbate particles at a given temperature [20]. The experimental data obtained were analyzed by Langmuir, Freundlich, Dubinin-Radushkevic, and Temkin adsorption isotherm models.

2. 5. Design of Experiment In order to examine the combined effect of the five different factors (independent variables): temperature, contact time, adsorbent dosage, particle size, and stirring speed on adsorption efficiency and derive a model, a central composite full factorial design of $2^5 = 32$ plus 6 centre points and (2 x 5 = 10) star points leading to a total of 48 experiments were performed. The coded values of the process variables were determined by the following equation:

$$x_i = \frac{X_i - X_0}{\Delta x} \quad (3)$$

where, x_i –coded value of I^{th} variable, X_i- un-coded value of the I^{th} test variable and X_0 - un-coded value of the I^{th} test variable at center point. The factors levels with the corresponding real values and the design matrix are shown in Table 1 along with experimental data and predicted responses. The matrix for the five variables was varied at five levels (-α, -1, 0, +1, and +α). As usual, the experiments were performed in random order to avoid systematic error. The regression analysis was performed to estimate the response function as a second-order polynomial:

$$Y = \beta_0 + \sum_{i=1}^{k} \beta_i X_i + \sum_{i=1}^{k} \beta_{ii} X_i^2 + \sum_{i=1,i<j}^{k-1} \sum_{j=2}^{k} \beta_{ij} X_i X_j \quad (4)$$

where, Y is the predicted response, β_i, β_{ii}, β_{ij} are coefficients estimated from regression. They represent the linear, quadratic and interactions of the independent variables on the response. The generated experimental data were analyzed using the Design Expert 8.0.7.1 trial version software by Statease Inc. USA and then interpreted. The analytical steps used include: analysis of variance (ANOVA), regression analysis, and response surface plots of the interaction effects of the factors to evaluate optimum conditions for the adsorption process. The linear, quadratic, and linear interactive effects of the process variables on the dye removal efficiency were calculated and their respective significant evaluated by ANOVA test. The *p*-value was used as the yardstick for measuring the significance of the regression coefficients, values of p less than 0.05 signified that the coefficient is significant. The experimental data were fitted to the second-order polynomial regression model and the adequacy of the model tested by the coefficient of determination (R^2) value as compared to the adjusted R^2 value.

3. RESULTS AND DISCUSSIONS

3. 1. Characterization of the Bentonite Adsorbent The results of the chemical analyses, surface area, and cation exchange capacity (CEC) are reported in Table 2, while the result of the pH point of zero charge (PZC) is reported in Figure 1. As can be observed from Table 2, the octahedral cations such as Al^{3+}, Fe^{3+}, and Mg^{2+}, reduced appreciably as the intensity of the acid treatment increased, while the tetrahedral cations, like Si^{4+}, increased with severity of treatment. The behavior showed by the Al_2O_3, Fe_2O_3, and MgO content with progressive acid treatment is related to the progressive dissolution of the bentonite minerals. The octahedral sheet destruction passes the cations into the solution, while the silica generated by the tetrahedral sheet remains in the solids, due to its insolubility. In literature, it is suggested that this free silica generated by the initial destruction of the tetrahedral sheet is polymerized by the effect of such high acid concentrations and is deposited on the undestroyed silicate fractions, protecting it from further attack. The cation exchange capacity [21] of the activated samples show that the exchange ability of the activated samples decreased as the concentration of the acid used in the activation increased. With the increase of concentration of sulphuric acid, the bentonite showed a gradual decrease of the CEC until dissolving with 1.5 mol L^{-1} H_2SO_4 acid. In treatment with 2.00 mol L^{-1} H_2SO_4 acid, as the SiO_2 content decreased, an increase of CEC was observed in comparison with the CEC observed with the sample treated with 1.5mol L^{-1}.

TABLE 1. Experimental design matrix with the experimental and predicted values of the response variable (dye removal efficiency, (%))

	Temperature, °C (A)		Contact Time, min (B)		Adsorbent dosage g/L (C)		Particle size, mm (D)		Stirring speed, rpm (E)		Dye removal (%)	
Run No.	Coded	Real	Coded	Real	Coded	Real	Coded	Real	Coded	Real	Exp.	Pred.
1	-1	30	-1	80	-1	0.1	-1	0.05	-1	200	67	61.34
2	+1	70	-1	80	-1	0.1	-1	0.05	-1	200	34	35.97
3	-1	30	+1	300	-1	0.1	-1	0.05	-1	200	68	65.14
4	+1	70	+1	300	-1	0.1	-1	0.05	-1	200	48	44.65
5	-1	30	-1	80	+1	0.5	-1	0.05	-1	200	70	67.84
6	+1	70	-1	80	+1	0.5	-1	0.05	-1	200	47	45.85
7	-1	30	+1	300	+1	0.5	-1	0.05	-1	200	60	63.51
8	+1	70	+1	300	+1	0.5	-1	0.05	-1	200	46	46.40
9	-1	30	-1	80	-1	0.1	+1	0.21	-1	200	30	34.23
10	+1	70	-1	80	-1	0.1	+1	0.21	-1	200	26	23.99
11	-1	30	+1	300	-1	0.1	+1	0.21	-1	200	47	45.16
12	+1	70	+1	300	-1	0.1	+1	0.21	-1	200	46	39.79
13	-1	30	-1	80	+1	0.5	+1	0.21	-1	200	48	44.35
14	+1	70	-1	80	+1	0.5	+1	0.21	-1	200	39	37.49
15	-1	30	+1	300	+1	0.5	+1	0.21	-1	200	50	47.16
16	+1	70	+1	300	+1	0.5	+1	0.21	-1	200	37	45.17
17	-1	30	-1	80	-1	0.1	-1	0.05	+1	400	58	56.37
18	+1	70	-1	80	-1	0.1	-1	0.05	+1	400	37	40.38
19	-1	30	+1	300	-1	0.1	-1	0.05	+1	400	64	64.55
20	+1	70	+1	300	-1	0.1	-1	0.05	+1	400	54	53.44
21	-1	30	-1	80	+1	0.5	-1	0.05	+1	400	62	66.25
22	+1	70	-1	80	+1	0.5	-1	0.05	+1	400	55	53.63
23	-1	30	+1	300	+1	0.5	-1	0.05	+1	400	66	66.30
24	+1	70	+1	300	+1	0.5	-1	0.05	+1	400	54	58.56
25	-1	30	-1	80	-1	0.1	+1	0.21	+1	400	46	37.39
26	+1	70	-1	80	-1	0.1	+1	0.21	+1	400	37	36.52
27	-1	30	+1	300	-1	0.1	+1	0.21	+1	400	47	52.69
28	+1	70	+1	300	-1	0.1	+1	0.21	+1	400	52	56.70
29	-1	30	-1	80	+1	0.5	+1	0.21	+1	400	42	50.89
30	+1	70	-1	80	+1	0.5	+1	0.21	+1	400	49	53.40
31	-1	30	+1	300	+1	0.5	+1	0.21	+1	400	60	58.06
32	+1	70	+1	300	+1	0.5	+1	0.21	+1	400	65	65.45
33	-2	2.43	0	190	0	0.3	0	0.13	0	300	50	52.52
34	+2	97.57	0	190	0	0.3	0	0.13	0	300	35	31.14
35	0	50	-2	-71.63	0	0.3	0	0.13	0	300	39	40.40
36	0	50	+2	451.63	0	0.3	0	0.13	0	300	62	59.26
37	0	50	0	190	-2	-0.18	0	0.13	0	300	33	39.26
38	0	50	0	190	+2	0.78	0	0.13	0	300	65	57.39
39	0	50	0	190	0	0.3	-2	-0.07	0	300	52	52.85
40	0	50	0	190	0	0.3	+2	0.33	0	300	31	28.81
41	0	50	0	190	0	0.3	0	0.13	-2	62.16	30	37.22
42	0	50	0	190	0	0.3	0	0.13	+2	537.84	64	55.44
43	0	50	0	190	0	0.3	0	0.13	0	300	90.4	89.80
44	0	50	0	190	0	0.3	0	0.13	0	300	89.4	89.80
45	0	50	0	190	0	0.3	0	0.13	0	300	89.9	89.80
46	0	50	0	190	0	0.3	0	0.13	0	300	90.2	89.80
47	0	50	0	190	0	0.3	0	0.13	0	300	89.8	89.80
48	0	50	0	190	0	0.3	0	0.13	0	300	90	89.80

TABLE 2. The chemical composition of the raw and activated bentonite samples as given by x-ray fluorescence, cation exchange capacity (CEC), and surface area

	Bentonite samples				
Chemical constituents	**NB0**	**NB0.5**	**NB1.0**	**NB1.5**	**NB2.0**
Al_2O_3	29.76	23.52	12.41	4.96	5.74
SiO_2	45.35	57.74	74.36	86.66	85.23
Fe_2O_3	14.81	10.64	7.49	4.42	4.98
MgO	1.96	1.63	1.06	0.52	0.07
Na_2O	0.86	0.67	0.27	0.11	0.05
K_2O	0.59	0.33	0.14	0.02	0.02
CaO	0.55	0.39	0.17	0.06	0.03
TiO_2	1.38	1.06	0.53	0.12	0.09
LOI	4.74	3.96	2.28	1.08	0.99
Total	100	99.94	98.71	97.95	92.2
CEC (meq/100g)	69	52	45	30	28
Surface area (m^2/g)	29.8	38.4	45.2	66.3	54.5

This is due to the removal of the exchangeable ions from the lattice of the clay samples by the acid hydrogen ion which occupies the vacant sites created by the removal of the octahedral and tetrahedral ions.

The surface area of the activated sample was determined using the ethylene glycol mono-ethyl-ether (EGME) method described by Carter et al. [22]. Results of the analysis showed that the surface area of the acid activated samples increased with an increase in acid concentration until a maximum surface area is reached after which it gradually decreased [23]. In this study, the surface area increased with an increase in acid concentration from 0.5M to 1.5M and decreased beyond 1.5M as shown in Table 2. This increase in surface area is attributed to the removal of impurities, replacement of exchangeable cations (K^+, Na^+, Ca^{2+}) with hydrogen ions and leaching of Al^{3+}, Fe^{3+}, and Mg^{2+} from the octahedral and tetrahedral sites in bentonite which exposes the edges of platelets [24]. The decrease in surface area beyond 1.5M concentration is attributed to the deeper penetration of acid into the voids and excessive leaching of Al^{3+}, Fe^{3+}, and Mg^{2+}, resulting in the collapse of layered structure and close packing of particles [25].

3. 1. 1. pH Point of Zero Charge of the Adsorbent (NB1.5)

The point of zero charge (pH_{PZC}) is the pH at which the total number of positive and negative charges on its surface becomes zero. The pH at the point of zero charge (pH_{PZC}) of NB1.5 was measured using the pH drift method [26]. It can be observed from Figure 1 that the surface charge of NB1.5 at pH 8.6 is zero. Hence, the pH at point of zero charge of the sorbent is 8.6. According to the literature, the adsorption of cations is favored at pH > pH_{PZC}, while the adsorption of anions is favored at pH < pH_{PZC}. Thus, the determination of this parameter is significant for the assessment of the sorption mechanism and the probable sorbate/sorbent interactions.

3. 1. 2. XRD Analyses of the Raw and NB1.5 Modified Bentonite

The XRD patterns of raw bentonite and acid activated bentonite are shown in Figures 2 and 3, respectively. Montmorillonite (M) was the main mineral; however, minor amounts of quartz (Q), chyrstoballitte (C) and calcium carbonate are present. These results are in accordance with literature publications. The strong diffraction peaks at $2\theta = 26.7°$ and 31.06° can be ascribed to the characteristic diffraction of quartz and chrystoballite impurities [27], respectively, which indicated the existence of quartz impurities.

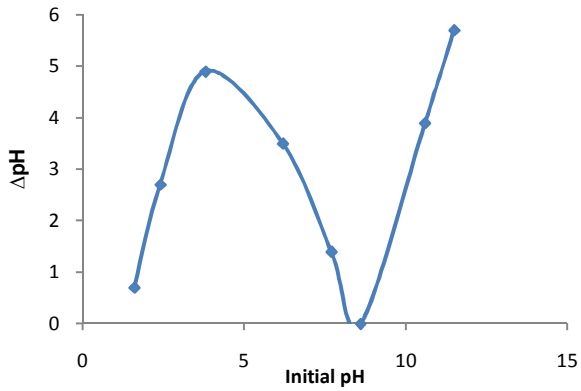

Figure 1. pH at the point of zero charge (pH_{PZC}).

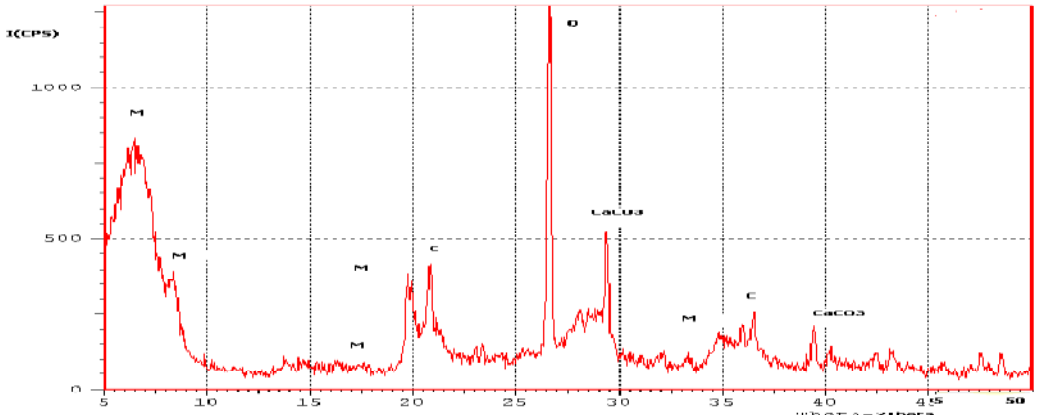

Figure 2. XRD image of raw bentonite sample.

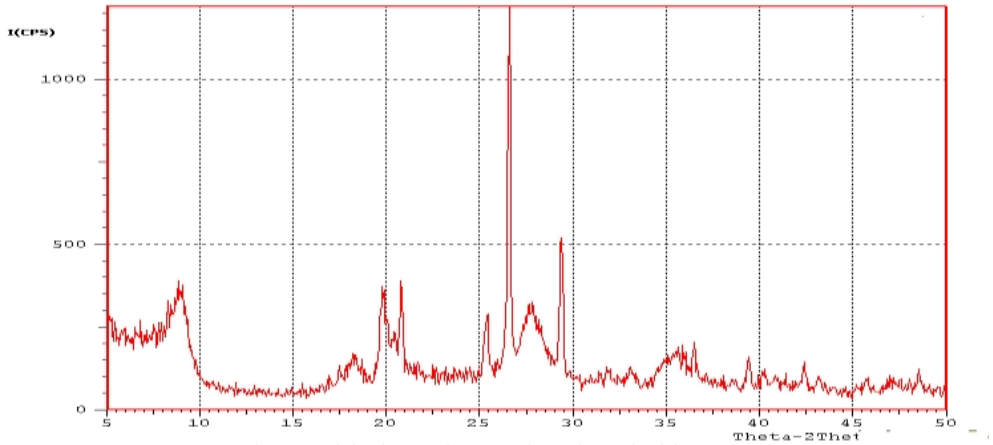

Figure 3. XRD image of the bentonite sample activated with 1.5 mol/L of H_2SO_4

In addition, the diffraction peaks at 2θ =21.6° and 36.4° reveal the presence of small amounts of calcites. After treated with 1.5 mol/L of H_2SO_4 solution, the characteristic peaks of montmorillonite, calcium carbonate, and chrystoballite almost disappeared, indicating that these impurities were removed. The diffraction peaks at 2θ = 7.45° are assigned to the (110) characteristic peaks of sepiolites [28, 29].

3. 2. Evaluation of Regression Model for Dye Removal Efficiency The correlation between the experimental process variables and the dye removal efficiency was evaluated using the CCRD modeling technique. Second order polynomial regression equation was fitted between the response (dye removal efficiency, (Y)) and the process variables: temperature (A), contact time (B), adsorbent dosage (C), particle size (D) and stirring speed (E). From Table 4, the ANOVA results showed that the quadratic model is suitable to analyze the experimental data. The model in terms of the coded values of the process parameters is given by:

$$Y = 89.80 - 4.49A + 3.96B + 3.81C - 5.05D + 3.83E + 1.22AB + 0.84AC + 3.78AD + 2.34AE - 2.03BC + 1.78BD + 1.09BE + 0.91CD + 0.84CE + 2.03DE - 8.48A^2 - 7.07B^2 - 7.33C^2 - 8.66D^2 - 7.69E^2 \quad (5)$$

To develop a statistically significant regression model, the significance of the regression coefficients was evaluated based on the p-values. The coefficient terms with p-values more than 0.05 are insignificant and are removed from the regression model. The analysis in Table 4 shows that all the linear terms; all the quadratic terms, and the interaction terms of temperature and particle size; temperature and stirring speed; contact time and adsorbent dosage; particle size and stirring speed; are significant model terms. The model reduces to Equation (6) after eliminating the insignificant coefficients.

$$Y = 89.80 - 4.49A + 3.96B + 3.81C - 5.05D + 3.83E + 3.78AD + 2.34AE - 2.03BC + 2.03DE - 8.48A^2 - 7.07B^2 - 7.33C^2 - 8.66D^2 - 7.69E^2 \quad (6)$$

The analysis of variance indicated that the quadratic polynomial model was significant and adequate to

represent the actual relationship between dye removal efficiency and the significant model variables as depicted by very small p-value (0.0000). The significance and adequacy of the established model was further elaborated by high value of R^2 (0.9476) and adj. R^2 value of 0.9088. This means that the model explains 94.76% of the variation in the experimental data. The adequate correlation between the experimental values of the independent variable and predicted values further showed the adequacy of the model as illustrated in Figure 4.

3. 3. Response Surface Estimation of Maximum Removal of Malachite Green from Solution The interactive effects of the process variables on the percent dye removal efficiency were studied by plotting three dimensional surface curves against any two independent variables, while keeping other variables at their central (0) level. The 3D curves of the response (dye removal efficiency) and contour plots from the interactions between the variables are shown in Figure 5 (a – j). The response surface curves were plotted to understand the interaction of the variables and to determine the optimum level of each variable for maximum response. The elliptical shape of the curves indicates good interaction of the two variables and circular shape indicates no interaction between the variables. The curves obtained in this study showed that there is relative significant interaction between all the variables. Results of the graphical representation of the interaction effects show that all the interaction terms have positive effect on the percentage dye removal, except the interaction of contact time and adsorbent dosage which has a negative effect on the response variable. Optimum conditions of malachite green removal using activated clay were also obtained from the response surface plots. The stationary point or central point is the point at which the slope of the contour is zero in all directions. The coordinates of the central point within the highest contour levels in each of the plots will correspond to the optimum values of the respective variables. The maximum predicted dye removal is indicated by the surface confined in the smallest curve of the contour diagram. The optimum values of the variables were: temperature, 70 ^{0}C; contact time, 229.68 min; adsorbent dosage, 0.36 g/L; particle size, 0.13 mm; and stirring speed, 344.76 rpm. The predicted response value (% dye removal) at these optimum values was 79.82 %. To confirm this optimum values, experiments were performed at these values and the experimental response value (% dye removal) was 80.04 %. This showed that the model correctly explains the influence of the process variables on the removal of malachite green from aqueous solution.

3. 4. Effect of Initial Dye Concentration The effect of initial dye concentration of malachite green on activated bentonite was examined over a concentration range of 100mg/l to 300mg/l at interval of 50mg/l. The results of the analyses are shown in Figure 6. The figure shows that initial dye concentration plays a vital role in the adsorption of dye by adsorbents. The amount of adsorbtion increased with an increase in initial dye concentration. An increase in amount of adsorbtion with an increase in dye concentration is due to the driving force that initial concentration provides to overcome the mass transfer resistance between the aqueous and solid phases. The adsorption rate was high at early adsorption period due to availability of large number of vacant site which increased the concentration gradient between the adsorbate in the solution and adsorbate on the adsorbent surface [30].

3. 5. Effect of pH The effect of pH on the adsorption rate of MG on NB1.5 activated bentonite was investigated in the pH range of 4.8 to 11.5 at 343K, 0.36g/L adsorbent dosage and 345 rpm stirring speed. Figure 7 shows the variation of the amount of adsorbtion with time at different pH value. The figure indicates that adsorption of MG increased with an increase in the pH value. This can be explained by considering the pH_{PZC} of the adsorbent – 8.6. As pH of the system decreased below the pH_{PZC} of the adsorbent, the number of negative charge of adsorbent sites decreased and the positive charge of surface sites increased, which did not favor the adsorption of cationic dyes due to electrostatic repulsion. At higher pH, negative charge of adsorbent sites increased, which enhances the adsorption of positive charge of dye cations through electrostatic forces of attraction [2].

3. 6. Adsorption Kinetic Studies The effect of contact time on the adsorption of malachite green on activated Ntezi bentonite was studied and the results show that adsorption increased with an increase in contact time. The experimental data were examined by pseudo-first-order, pseudo-second-order, Elovich, and intra-particle diffusion kinetic equations to understand the dynamics and mechanism of the adsorption process.

3. 6. 1. Pseudo-first-order Kinetic Model A simple pseudo-first order equation was used and it is given by

$$\frac{dq_t}{dt} = k_1 (q_e - q_t) \quad (7)$$

where, q_e and q_t are the amount of MG adsorbed at equilibrium and at time t (min), respectively, and k_1 is the rate constant of the pseudo-first order adsorption process [31, 32].

TABLE 3. Analysis of variance (ANOVA)

Source	Coefficient	Sum of Squares	df	Mean Square	F Value	p-value Prob > F
Model	89.80	14000.69	20	700.03	24.41	< 0.0001
A-Temperature	-4.49	874.98	1	874.98	30.51	< 0.0001
B-Contact time	3.96	680.66	1	680.66	23.74	< 0.0001
C-Asorbent dosage	3.81	629.39	1	629.39	21.95	< 0.0001
D-Particle size	-5.05	1106.75	1	1106.75	38. 60	< 0.0001
E-Stirring speed	3.83	635.17	1	635.17	22.15	< 0.0001
AB	1.22	47.53	1	47.53	1.66	0.2089
AC	0.84	22.78	1	22.78	0.79	0.3806
AD	3.78	457.53	1	457.53	15.96	0.0004
AE	2.34	175.78	1	175.78	6.13	0.0199
BC	-2.03	132.03	1	132.03	4.60	0.0410
BD	1.78	101.53	1	101.53	3.54	0.0707
BE	1.09	38.28	1	38.28	1.33	0.2580
CD	0.91	26.28	1	26.28	0.92	0.3469
CE	0.84	22.78	1	22.78	0.79	0.3806
DE	2.03	132.03	1	132.03	4.60	0.0410
A^2	-8.48	3688.56	1	3688.56	128.63	< 0.0001
B^2	-7.07	2560.95	1	2560.95	89.31	< 0.0001
C^2	-7.33	2756.75	1	2756.75	96.14	< 0.0001
D^2	-8.66	3843.93	1	3843.93	134.05	< 0.0001
E^2	-7.69	3029.04	1	3029.04	105.63	< 0.0001
Residual		774.23	27	28.68		
Lack of Fit		773.64	22	35.17	295.51	< 0.0001
Pure Error		0.60	5	0.12		
Cor Total		14774.92	47			

Std. dev.: 5.35; mean: 54.41; C.V.: 9.84%; PRESS: 3045.76; R^2: 0.9476; adj. R^2: 0.9088; predicted R^2: 0.7939; adeq. Precision: 18.581

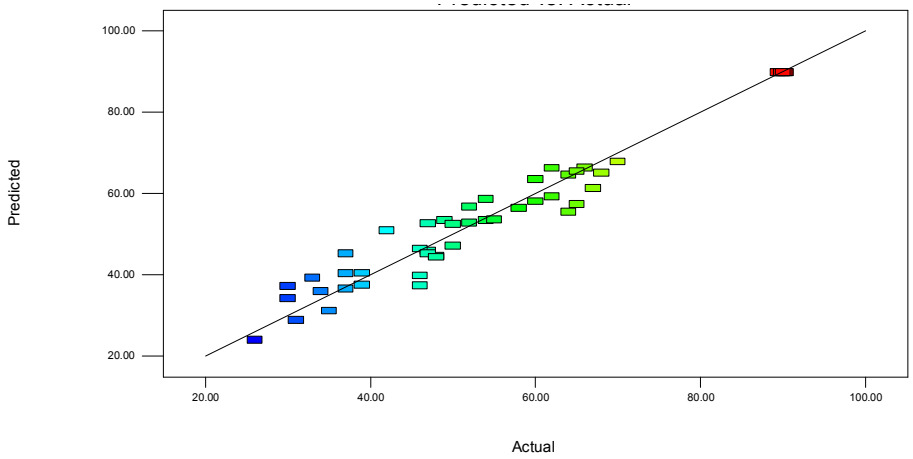

Figure 4. Plot of the predicted dye removal efficiency versus the actual experimental value

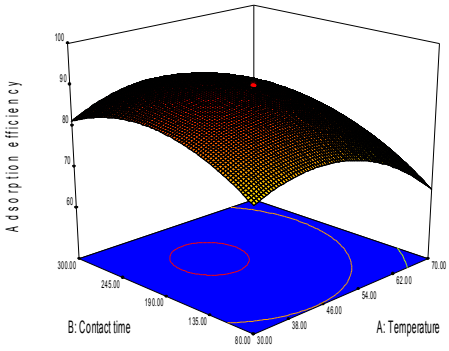
Adsorption efficiency
B: Contact time
A: Temperature

(a)

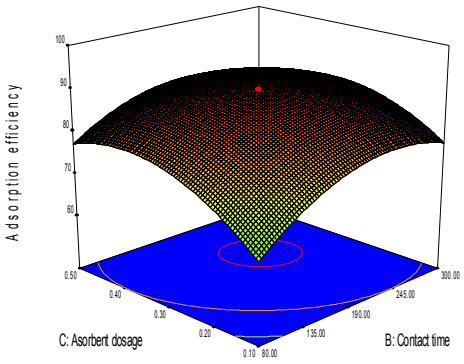
Adsorption efficiency
C: Asorbent dosage
B: Contact time

(e)

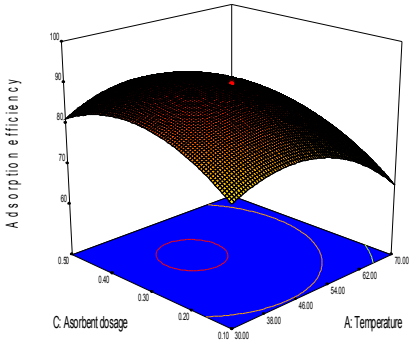
Adsorption efficiency
C: Asorbent dosage
A: Temperature

(b)

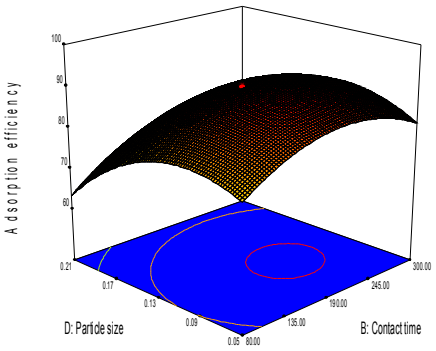
Adsorption efficiency
D: Particle size
B: Contact time

(f)

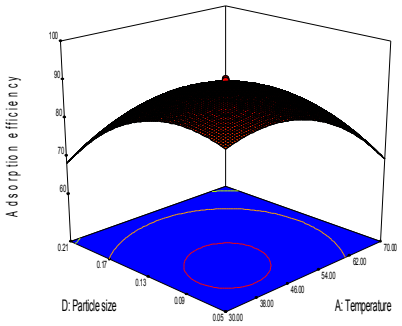
Adsorption efficiency
D: Particle size
A: Temperature

(c)

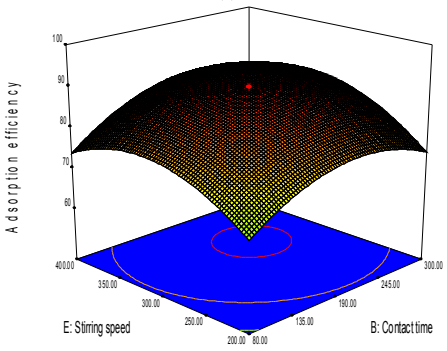
Adsorption efficiency
E: Stirring speed
B: Contact time

(g)

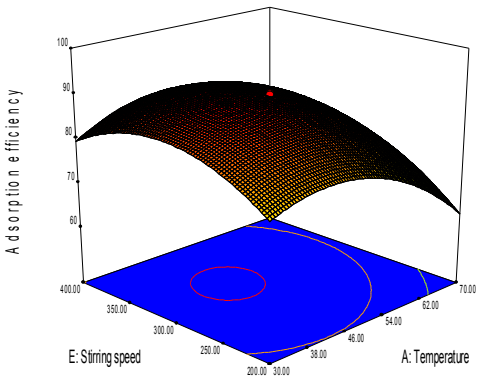
Adsorption efficiency
E: Stirring speed
A: Temperature

(d)

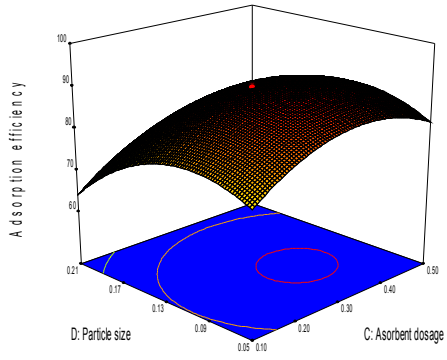
Adsorption efficiency
D: Particle size
C: Asorbent dosage

(h)

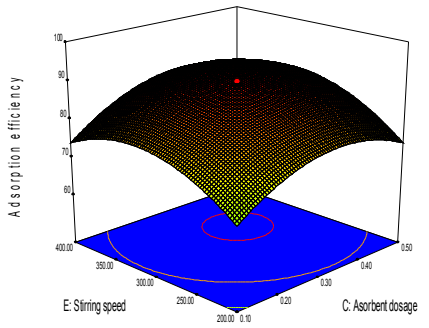

(i)

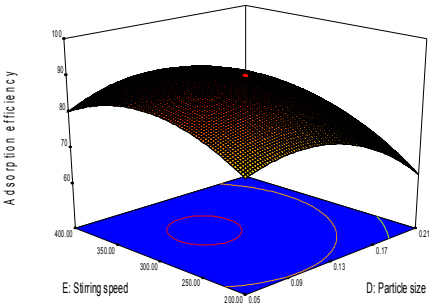

(j)

Figure 5. 3D plot of the effects of (a) contact time and temperature; (b) adsorbent dosage and temperature; (c) particle size and temperature; (d) stirring speed and temperature; (e) adsorbent dosage and contact time; (f) particle size and contact time; (g) stirring speed and contact time; (h) particle size and adsorbent dosage; (i) stirring speed and adsorbent dosage; and (j) stirring speed and particle size; on adsorption efficiency of MG on NB1.5 activated Ntezi bentonite.

The linear form of the equation is given as:

$$\log(q_e - q_t) = \log q_e - \frac{k_1}{2.303}\, t \tag{8}$$

The values of k_1 and q_e were calculated from the slope and intercept of the linear plot of *log* $(q_e - q_t)$ versus t and are given in Table 4.

3. 6. 2. Pseudo-second order Kinetic Model The corresponding pseudo-second order rate equation [33] is given as,

$$\frac{t}{q_t} = \frac{1}{k_2 q_e^2} + \frac{t}{q_e} \tag{9}$$

where, k_2 is the rate constant for the pseudo-second order adsorption process (g mg^{-1} min^{-1}). The slope and intercept of the plot of t/q_t versus t (Figure 8) were used to calculate the values of q_e and k_2 as presented in Table 4. The value of the regression coefficient calculated from the plot of the second-order kinetic plot shows that it best fitted with the experimental data and can be used to describe the adsorption of MG on to activated Ntezi bentonite.

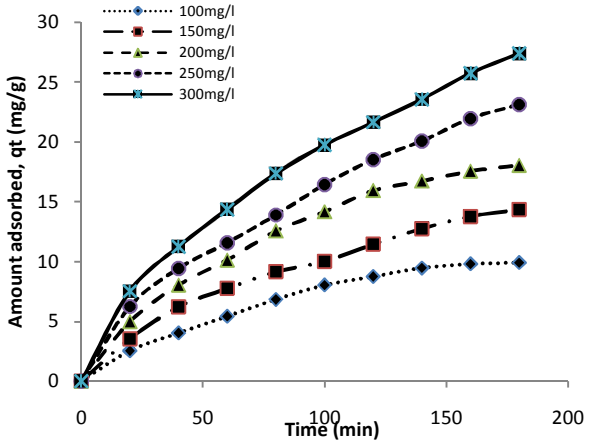

Figure 6. Effect of initial dye concentration on MG adsorption onto NB1.5 activated bentonite

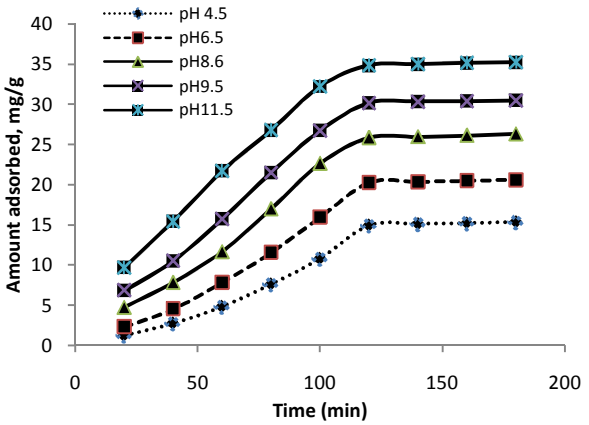

Figure 7. Effect of solution pH on dye adsorption on NB1.5 activated bentonite

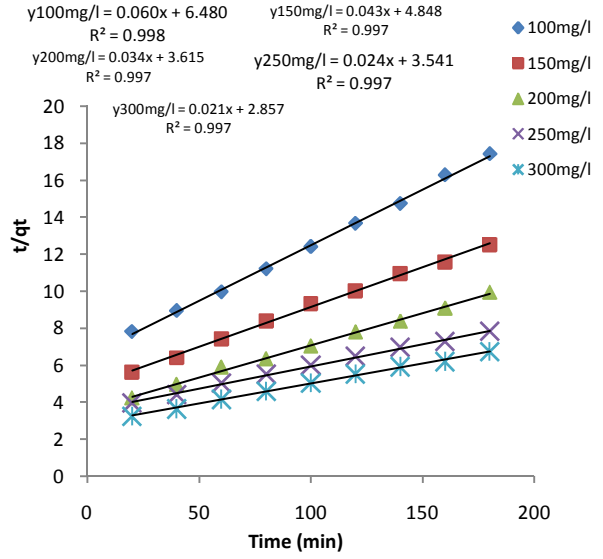

Figure 8. Plot of the pseudo-second order kinetic model for MG adsorption on NB1.5.

3. 6. 3. Elovich Kinetic Model The Elovich model is presented by the following equation:

$$q_t = \frac{1}{\beta}\ln \alpha\beta + \frac{1}{\beta}\ln t \quad (10)$$

where, α is the initial adsorption rate (mg/g/min) and β is the desorption constant (g/mg). The slope and intercept of the plot of q_t versus $ln\ t$ were used to calculate the values of the constants α and β as shown in Table 4. The value of the determination coefficient obtained from the linear plot of Elovich models are not high ($R^2 < 0.979$), suggesting that the applicability of this model to describe the adsorption process of MG on to activated Ntezi bentonite is not feasible.

3. 6. 4. Bangham's Equation Bangham's model tests is applied if pore diffusion is the only rate controlling step of an adsorption process. The model can be represented by the following equation

$$\log\left[log\left(\frac{c_0}{c_0 - q_t m}\right)\right] = \log\left(\frac{k_0 m}{2.303V}\right) + \sigma \log t \quad (11)$$

where, c_o, mg/L, is the initial adsorbate concentration in the liquid phase; q_t, mg/g – adsorbate concentration in the solid phase at time t, min; m, g/L – adsorbate concentration; V, L – solution volume; k_o, L/g, and σ ($\sigma < 1$) – Bangham's equation parameters. The values of the constants were calculated from the slope and intercept of the plot of $log\ [log\ (c_o / (c_o - q_t\ m))]$ versus $log\ t$.

3. 6. 5. Intra-particle Diffusion Study The adsorption mechanism of adsorbate on to adsorbent follows three steps: (1) transport of adsorbate from the boundary film to the external surface of the adsorbent; (2) adsorption at a site on the surface; (3) intra-particle diffusion of the adsorbate molecules to an adsorption site by a pore diffusion process. The slowest of the three steps controls the overall rate of the process. The possibility of intra-particle diffusion was explored by using an intra-particle diffusion model. The intra-particle diffusion varies with square root of time and is given [33, 34] as,

$$q_t = k_{id} t^{1/2} + C_i \quad (12)$$

where, q_t is the amount of adsorbtion at time t, $t^{1/2}$ is the square root of the time, k_{id} is the intra-particle diffusion rate constant (mg/g $min^{1/2}$), and C_i is the intercept at stage i and is related to the thickness of the boundary layer. Large C_i represents the greater effect of the boundary layer on molecule diffusion. The intra-particle diffusion rate constant was determined from the slope of the linear gradients of the plot q_t versus $t^{1/2}$ as shown in Figure 9 and their values are presented in Table 4. The intraparticle diffusion process is controlled by the diffusion of ions within the adsorbent.

The commensurable and relatively high values of R_B^2 and R_i^2 for both studied systems, calculated by the Bangham's. The intra-particle diffusion models proved the significant role of intra-particle diffusion as one of the probable rate controlling mechanisms during malachite green adsorption on activated bentonite.

3. 7. Adsorption Isotherm Equilibrium study on adsorption provides information on the capacity of the adsorbent. An adsorption isotherm is characterized by certain constant values, which express the surface properties and affinity of the adsorbent, and could also be used to compare the adsorptive capacities of the adsorbent for different pollutants. The adsorption isotherms of MG on NB1.5 activated bentonite were studied and the equilibrium data analyzed using Langmuir, Freundlich, Temkin, and Dubinin-Radushkevic models.

3. 7. 1. Langmuir Isotherm The Langmuir isotherm model is based on the fact that uptake of dye molecules occurs on a homogeneous surface by monolayer adsorption with no interaction between adsorbed molecules, with homogeneous binding sites, equivalent sorption energies, and no interaction between adsorbed species. The model is given by the following linear equation:

$$\frac{C_e}{q_e} = \frac{1}{q_m K_L} + \frac{C_e}{q_m} \quad (13)$$

where, C_e is the equilibrium concentration (mg/L); q_e is the amount of dye ion adsorbed (mg/g); q_m is the Langmuir constant for adsorption capacity (mg/g); K_L is sorption equilibrium constant (L/g).

The values of q_m and K_L were evaluated from the slope and intercept of the plot of C_e/q_e versus C_e as shown in Figure 10 [35, 36] and are given in Table 5.

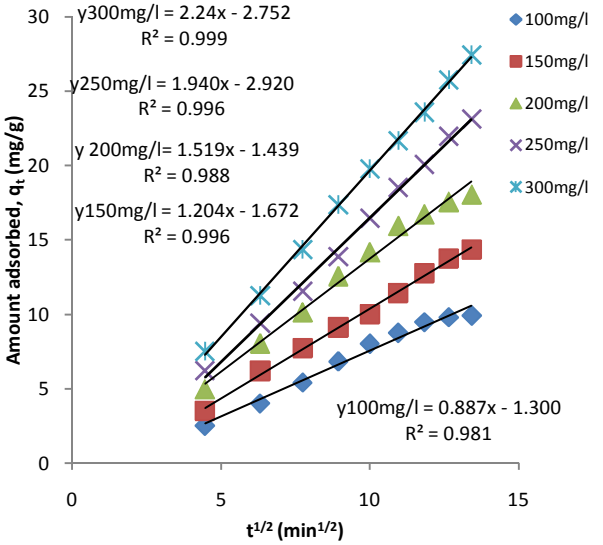

Figure 9. Plot of the intra-particle kinetic model for MG adsorption on NN1.5 bentonite

TABLE 4. Parameters of the Pseudo-first-order, Pseudo-second-order, Elovich, Bangham, and Intra-particle kinetic models together with their regression coefficients

Kinetic models	Parameters	Initial dye concentration				
		100mg/l	150mg/l	200mg/l	250mg/l	300mg/l
Pseudo-first-order	k_1 (min^{-1})	0.0276	0.0184	0.0207	0.0161	0.0161
	q_e (mg/g)	20.80	19.72	26.98	30.62	33.04
	R_1^2	0.907	0.902	0.949	0.918	0.939
Pseudo-second-order	k_2 (g/mg min)	5.56×10^{-4}	3.81×10^{-4}	3.20×10^{-4}	1.63×10^{-4}	1.54×10^{-4}
	q_e (mg/g)	16.67	23.26	29.41	41.67	47.62
	R_2^2	0.998	0.997	0.997	0.997	0.997
Elovich	B	0.271	0.202	0.158	0.126	0.109
	α (mg/g min)	0.314	0.437	0.614	0.699	0.850
	R_E^2	0.979	0.974	0.985	0.957	0.969
Bangham	k_0 (mol/g)	5.81×10^{-4}	3.04×10^{-4}	2.64×10^{-4}	1.96×10^{-4}	2.11×10^{-4}
	σ	0.424	0.535	0.561	0.611	0.596
	R_B^2	0.996	0.988	0.993	0.994	0.999
Intra-particle	K_p (mg/g $min^{0.5}$)	0.887	1.204	1.519	1.940	2.240
	C	-1.300	-1.672	-1.439	-2.920	-2.752
	R_i^2	0.981	0.996	0.988	0.996	0.999

A further analysis of the Langmuir equation can be made on the basis of a dimensionless equilibrium parameter, R_L [37] also known as the separation factor, given by

$$R_L = \frac{1}{(1+ K_L C_e)} \quad (14)$$

The value of R_L lies between 0 and 1 for favorable adsorption, while $R_L > 1$ represents unfavorable adsorption, and $R_L = 1$ represents linear adsorption while the adsorption process is irreversible if $R_L = 0$. Results of R_L calculated from this study (shown in Figure 11) lies between 0.056 and 0.962 and this is consistent with the requirement for favorable adsorption of MG on to activated Ntezi bentonite.

3. 7. 2. Freundlich Isotherm Freundlich isotherm assumes that the uptakes of metal ions occur on a heterogeneous surface by multilayer adsorption and that the amount of adsorbate adsorbed increases infinitely with an increase in concentration. It is a most popular model for a single solute system, based on the distribution of solute between the solid phase and aqueous phase at equilibrium [38]. The Freundlich equation is expressed as

$$q_e = K_f C_e^{1/n} \quad (15)$$

where, K_f is the measure of adsorption capacity and n is the adsorption intensity. Linear form of Freundlich equation [39] is,

$$\log q_e = \log K_f + \frac{1}{n} \log C_e \quad (16)$$

where, q_e is the amount of adsorbtion (mg/g), C_e is the equilibrium concentration of adsorbate (mg/L) and K_f and n are the Freundlich constants related to the adsorption capacity and adsorption intensity, respectively.

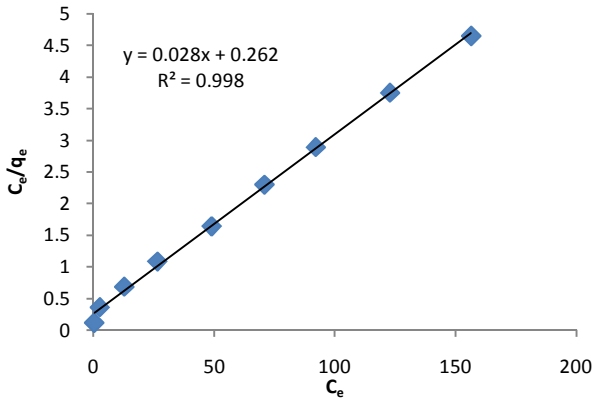

Figure 10. Plot of the Langmuir isotherm for the MG adsorption on to NB1.5 bentonite.

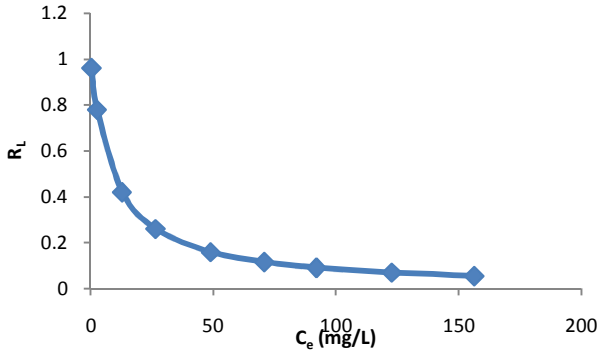

Figure 11. Plot of separation factor, R_L versus C_e.

A plot of *log* q_e *vs log* C_e gives a linear trace with a slope of *1/n* and intercept of *log* K_f and the results are also given in Table 5. When *1/n >1.0*, the change in adsorbed metal ion concentration is greater than the change in the metal ion concentration in solution.

3. 7. 3. Temkin Isotherm Model The Temkin isotherm model [40] has been developed on the concept of chemisorptions and assumes that the heat of adsorption of the sorbate molecules decreases linearly with adsorbent layer coverage due to adsorbate-adsorbent interactions. The equation and its linearized form are represented as follows:

$$q_e = \frac{RT}{b_T} \ln(K_T C_e) \quad (17)$$

$$q_e = B_1 \ln K_T + B_1 \ln C_e \quad (18)$$

where, $B_1 = RT/b_T$; b_T, *mol* kJ^{-1}, is the Temkin isotherm constant; K_T, mol g^{-1}, is the equilibrium binding constant; *T*, *K*, the temperature and *R* (8.314×10^{-3} kJ mol^{-1} K^{-1}) the universal gas constant. The isotherm parameters, b_T and K_T, can be calculated from the slope and intercept of the linear plot of q_e versus *ln* C_e.

3. 7. 4. Dubinin-Radushkevich Isotherm The D-R equation has been widely used to explain energetic heterogeneity of solid at low coverage as monolayer regions in micro-pores. The equation is given by

$$\ln q_e = \ln X_m - \beta\varepsilon^2 \quad (19)$$

where, β is the activity coefficient related to mean adsorption energy, X_m the maximum of adsorption capacity and ε is the Polangi potential, which is equal to

$$\varepsilon = RT \ln(\frac{1}{C_e}) \quad (20)$$

where, *R* and *T* are the gas constant (kJ/mol/K) and temperature (K), respectively.
The adsorption energy *E* expressed as;

$$E = -\frac{1}{(-2\beta)^{0.5}} \quad (21)$$

reveals the nature of adsorption. If the value of adsorption energy *E* ranged between -1 and -8 kJ/mol, adsorption process is physical, and if the value of E ranged between -9 and -16 kJ/mol, it is chemical adsorption. The parameters of the D-R equation were calculated from the slope and intercept of the linear plot of *ln qe* versus ε^2 and are given in Table 5.

The adsorption energy *E* value obtained -10.00kJ/mol showed that the adsorption of MG on to activated Ntezi bentonite is a chemical process.

The good fit of the experimental data and the determination coefficient closer to unity indicated the applicability of the Langmuir isotherm model to describe the adsorption of MG on to activated Ntezi bentonite.

TABLE 5. Langmuir, Freundlich, Temkin, and Dubinin-Radushkevich isotherm parameters for adsorption of MG on to activated Ntezi bentonite

Langmuir isotherm				Freundlich isotherm			Temkin isotherm			Dubinin-Radushkevich isotherm			
q_m (mg/g)	K_L (L/mg)	R_L	R^2	K_f (mg/g)	n	R^2	K_T (mol/g)	b_T (mol/kJ)	R^2	X_m (mg/g)	B (10^{-9})	E (kJ/mol)	R^2
35.71	0.107	0.056 to 0.962	0.998	11.830	4.930	0.989	17.15	0.710	0.933	12.807	5	-10	0.920

TABLE 6. Effect of temperature on the sorption of MG on to activated Ntezi bentonite

Temperature, (K)	Liquid-phase conc. of MG, C_e (mg/L)	Amount adsorbed, q (mg/g)	MG Removed, (%)
313	29.5	7.05	55.2
323	18.8	8.12	67.7
333	7.4	9.26	79.6
343	0.8	9.92	87.3

3. 8. Adsorption Thermodynamics The thermodynamics of an adsorption process is obtained from a study of the influence of temperature on the process. Temperature effect has been studied for the adsorption of MG ions by NB1.5 activated Ntezi bentonite. It has been found that the adsorption capacity increased from 7.05 mg/g to 9.92 mg/g (Table 6) as the temperature was increased from 313 K to 343 K at MG ion concentration of 100 mg/L, pH 8.6 and the other conditions were kept constant at optimum values. This indicates that the adsorption reaction was endothermic in nature. The enhancement in the adsorption capacity may be due to the chemical interaction between adsorbate and adsorbent, creation of some new adsorption sites or the increased rate of intra-particle diffusion of MG ions into the pores of tshe adsorbent at higher temperatures [34].
The standard Gibb's energy was,

$$\Delta G^\circ = -RT \ln K_c \quad (22)$$

K_c represents the ability of the adsorbent to retain the adsorbate and extent of movement of the adsorbate within the solution [18]. The values of K_c can be deduced from the relationship,

$$K_c = \frac{q_e}{C_e} \quad (23)$$

where, q_e is the amount adsorbed on solid phase at equilibrium and C_e is the equilibrium concentration of metal ion in the solution. Other thermodynamic parameters such as change in standard enthalpy (ΔH°) and standard entropy (ΔS°) were determined using the Van't Hoff's equation [41].

$$\ln K_c = \frac{\Delta S}{R} - \frac{\Delta H}{RT} \quad (24)$$

The values of ΔH° and ΔS° were obtained from the slope and intercept of the Van't Hoff's plot of $ln\ k_c$ versus $1/T$ as shown in Figure 12, positive value of ΔH° indicates that the adsorption process is endothermic. The negative values of ΔG° reflect the feasibility of the process and the values become more negative with increase in temperature. Standard entropy determines the disorderliness of the adsorption at solid–liquid interface. Thermodynamic parameters are summarized in Table 7. The positive value of ΔS° shows increasing randomness at the solid/liquid interface during the adsorption of MG ions on activated bentonite.

TABLE 7. Thermodynamic parameters of adsorption of MG on to NB1.5 activated bentonite

Temperature K	ΔG° kJ/mol	ΔH° kJ/mol	ΔS° J/mol K
313	-0.222	6.230	0.200
323	-0.382		
333	-0.620		
343	-0.813		

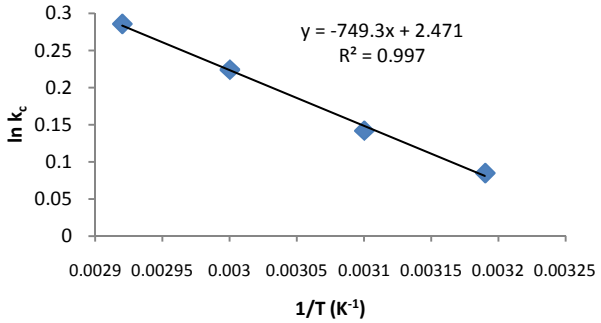

Figure 12. Plot of ln k_c versus 1/T.

4. CONCLUSIONS

In this study, bentonite from Ntezi was successfully activated with different concentrations of sulphuric acid solution. It was observed that the physicochemical properties such as surface area, cation exchange capacity, and sorption capacity increased as the acid concentration increased up to 1.5mol/l and above this the surface area decreased due to collapse of the clay structure. Results of the optimization studies revealed that the optimum operation conditions for the removal of malachite green from aqueous solution using activated bentonite were: temperature, 70 ^{0}C; contact time, 229.68 min; adsorbent dosage, 0.36g/L; particle size, 0.13mm; and stirring speed, 344.76 rpm. The removal of MG ions with an initial concentration of 100mg/g was found to be 99.25% after shaking for 220 min at constant temperature of 343 K. The experimental data for the adsorption process were well fitted to the Langmuir adsorption isotherm model relative to the fit of Freundlich, Temkin, and Dubinin-Radushkevich models. The kinetic analysis showed that adsorption of MG ions obeyed the pseudo-second-order kinetic equation. The increase in the adsorption capacity observed with increasing temperature showed that the adsorption process was chemical in nature, spontaneous and endothermic as confirmed by the evaluation of the relevant thermodynamic parameters, viz. ΔG°, ΔH°, and ΔS°. Results from this study has shown that Ntezi bentonite can be used as a low-cost, readily available, and easily prepared sorbent for the effective removal of MG from aqueous solution.

5. REFERENCES

1. Zhang, J., Li, Y., Zhang, C. and Jing, Y., "Adsorption of malachite green from aqueous solution onto carbon prepared from arundo donax root", ***Journal of Hazardous Materials***, Vol. 150, No. 3, (2008), 774-782.
2. F., B.A. and C., O., "Adsorption of cationic dye from aqueous solution by clay as an adsorbent: Thermodynamic and kinetic studies", ***Journal of the Chemical Society of Pakistan***, Vol. 34, No. 4, (2012), 896 - 906.

3. Gu, X.H., Zhou, J.T., Zhang, A.L. and Liu, G.F., "Treatment of hyper-saline wastewater loaded with phenol by the combination of adsorption and an offline bio-regeneration system", ***Journal of Chemical Technology and Biotechnology***, Vol. 83, No. 7, (2008), 1034-1040.
4. Crini, G., "Non-conventional low-cost adsorbents for dye removal: A review", ***Bioresource Technology***, Vol. 97, No. 9, (2006), 1061-1085.
5. Bhatnagar, A. and Jain, A., "A comparative adsorption study with different industrial wastes as adsorbents for the removal of cationic dyes from water", ***Journal of Colloid and Interface Science***, Vol. 281, No. 1, (2005), 49-55.
6. Shi, B., Li, G., Wang, D., Feng, C. and Tang, H., "Removal of direct dyes by coagulation: The performance of preformed polymeric aluminum species", ***Journal of Hazardous Materials***, Vol. 143, No. 1, (2007), 567-574.
7. Unuabonah, E.I., Adebowale, K.O. and Dawodu, F.A., "Equilibrium, kinetic and sorber design studies on the adsorption of aniline blue dye by sodium tetraborate-modified kaolinite clay adsorbent", ***Journal of Hazardous Materials***, Vol. 157, No. 2, (2008), 397-409.
8. McKay, G., Otterburn, M.S. and Aga, J.A., "Fuller's earth and fired clay as absorbents for dyestuffs external mass transport processes during adsorption", ***Water, Air, and Soil Pollution***, Vol. 26, No. 2, (1985), 149-161.
9. Šćiban, M., Klašnja, M. and Škrbić, B., "Adsorption of copper ions from water by modified agricultural by-products", ***Desalination***, Vol. 229, No. 1, (2008), 170-180.
10. Kabra, K., Chaudhary, R. and Sawhney, R.L., "Treatment of hazardous organic and inorganic compounds through aqueous-phase photocatalysis: A review", ***Industrial & Engineering Chemistry Research***, Vol. 43, No. 24, (2004), 7683-7696.
11. Santhy, K. and Selvapathy, P., "Removal of reactive dyes from wastewater by adsorption on coir pith activated carbon", ***Bioresource Technology***, Vol. 97, No. 11, (2006), 1329-1336.
12. Monvisade, P. and Siriphannon, P., "Chitosan intercalated montmorillonite: Preparation, characterization and cationic dye adsorption", ***Applied Clay Science***, Vol. 42, No. 3, (2009), 427-431.
13. An, J.-H. and Dultz, S., "Adsorption of tannic acid on chitosan-montmorillonite as a function of ph and surface charge properties", ***Applied Clay Science***, Vol. 36, No. 4, (2007), 256-264.
14. Qu, J., "Research progress of novel adsorption processes in water purification: A review", ***Journal of Environmental Sciences***, Vol. 20, No. 1, (2008), 1-13.
15. Al-Asheh, S., Banat, F. and Abu-Aitah, L., "Adsorption of phenol using different types of activated bentonites", ***Separation and Purification Technology***, Vol. 33, No. 1, (2003), 1-10.
16. Kara, M., Yuzer, H., Sabah, E. and Celik, M., "Adsorption of cobalt from aqueous solutions onto sepiolite", ***Water Research***, Vol. 37, No. 1, (2003), 224-232.
17. Chen, R., Peng, F. and Su, S., "Synthesis and characterization of novel swelling tunable oligomeric poly (styrene-co-acrylamide) modified clays", ***Journal of Applied Polymer Science***, Vol. 108, No. 4, (2008), 2712-2717.
18. Lian, L., Guo, L. and Guo, C., "Adsorption of congo red from aqueous solutions onto ca-bentonite", ***Journal of Hazardous Materials***, Vol. 161, No. 1, (2009), 126-131.
19. Özdemir, A. and Keskin, C.S., "Removal of a binary dye mixture of congo red and malachite green from aqueous solutions using a bentonite adsorbent", ***Clays and Clay Minerals***, Vol. 57, No. 6, (2009), 695-705.
20. Treybal, R.E. and Treybal Robert, E., "Mass-transfer operations, McGraw-Hill New York, Vol. 3, (1968).
21. Harrison, D.J. and Bloodworth, A., "Industrial minerals laboratory manual, British Geological Survey, (1994).
22. Carter, D., Heilman, M. and Gonzalez, C., "Ethylene glycol monoethyl ether for determining surface area of silicate minerals", ***Soil Science***, Vol. 100, No. 5, (1965), 356-360.
23. Pushpaletha, P., Rugmini, S. and Lalithambika, M., "Correlation between surface properties and catalytic activity of clay catalysts", ***Applied Clay Science***, Vol. 30, No. 3, (2005), 141-153.
24. Tsai, W.-T., Hsu, H.-C., Su, T.-Y., Lin, K.-Y., Lin, C.-M. and Dai, T.-H., "The adsorption of cationic dye from aqueous solution onto acid-activated andesite", ***Journal of Hazardous Materials***, Vol. 147, No. 3, (2007), 1056-1062.
25. Korichi, S., Elias, A. and Mefti, A., "Characterization of smectite after acid activation with microwave irradiation", ***Applied Clay Science***, Vol. 42, No. 3, (2009), 432-438.
26. Hameed, B., "Evaluation of papaya seeds as a novel non-conventional low-cost adsorbent for removal of methylene blue", ***Journal of Hazardous Materials***, Vol. 162, No. 2, (2009), 939-944.
27. Foletto, E., Volzone, C. and Porto, L.M., "Performance of an argentinian acid-activated bentonite in the bleaching of soybean oil", ***Brazilian Journal of Chemical Engineering***, Vol. 20, No. 2, (2003), 139-145.
28. Giustetto, R., Wahyudi, O., Corazzari, I. and Turci, F., "Chemical stability and dehydration behavior of a sepiolite/indigo maya blue pigment", ***Applied Clay Science***, Vol. 52, No. 1, (2011), 41-50.
29. Dikmen, S., Yilmaz, G., Yorukogullari, E. and Korkmaz, E., "Zeta potential study of natural-and acid-activated sepiolites in electrolyte solutions", ***The Canadian Journal of Chemical Engineering***, Vol. 90, No. 3, (2012), 785-792.
30. Zohra, B., Aicha, K., Fatima, S., Nourredine, B. and Zoubir, D., "Adsorption of direct red 2 on bentonite modified by cetyltrimethylammonium bromide", ***Chemical Engineering Journal***, Vol. 136, No. 2, (2008), 295-305.
31. Ho, Y. and McKay, G., "The sorption of lead (ii) ions on peat", ***Water Research***, Vol. 33, No. 2, (1999), 578-584.
32. Öztürk, N. and Kavak, D., "Adsorption of boron from aqueous solutions using fly ash: Batch and column studies", ***Journal of Hazardous Materials***, Vol. 127, No. 1, (2005), 81-88.
33. Ho, Y.-S. and McKay, G., "Sorption of dye from aqueous solution by peat", ***Chemical Engineering Journal***, Vol. 70, No. 2, (1998), 115-124.
34. Karthikeyan, T., Rajgopal, S. and Miranda, L.R., "Chromium (vi) adsorption from aqueous solution by *hevea brasilinesis* sawdust activated carbon", ***Journal of Hazardous Materials***, Vol. 124, No. 1, (2005), 192-199.
35. Langmuir, I., "The constitution and fundamental properties of solids and liquids. Ii. Liquids. 1", ***Journal of the American Chemical Society***, Vol. 39, No. 9, (1917), 1848-1906.
36. Aluyor, E., Oboh, I. and Obahiagbon, K., "Equilibrium sorption isotherm for lead (pb) ions on hydrogen peroxide modified rice hulls", ***International Journal of Physical Sciences***, Vol. 4, No. 8, (2009), 423-427.
37. Hall, K., Eagleton, L., Acrivos, A. and Vermeulen, T., "Pore-and solid-diffusion kinetics in fixed-bed adsorption under constant-pattern conditions", ***Industrial & Engineering Chemistry Fundamentals***, Vol. 5, No. 2, (1966), 212-223.
38. Sivakumar, P. and Palanisamy, P., "Adsorption studies of basic red 29 by a nonconventional activated carbon prepared from euphorbia antiquorum l", ***International Journal of ChemTech Research***, Vol. 1, No. 3, (2009).
39. Babel, S. and Kurniawan, T.A., "Cr (vi) removal from synthetic wastewater using coconut shell charcoal and commercial

activated carbon modified with oxidizing agents and/or chitosan", ***Chemosphere***, Vol. 54, No. 7, (2004), 951-967.

40. Temkin, M. and Pyzhev, V., "Kinetics of ammonia synthesis on promoted iron catalysts", ***Acta physiochim. URSS***, Vol. 12, No. 3, (1940), 217-222.

41. Demiral, H., Demiral, İ., Tümsek, F. and Karabacakoğlu, B., "Adsorption of chromium (vi) from aqueous solution by activated carbon derived from olive bagasse and applicability of different adsorption models", ***Chemical Engineering Journal***, Vol. 144, No. 2, (2008), 188-196.

Adsorption of Malachite Green from Aqueous Solution using Activated Ntezi Clay: Optimization, Isotherm and Kinetic Studies

R. O. AJEMBA

Department of Chemical Engineering, Nnamdi Azikiwe University, Awka, Anambra, Nigeria

P A P E R I N F O

Paper history:
Received 10 August 2013
Accepted in revised form 12 December 2013

Keywords:
Adsorption
Equilibrium
Kinetics
Isotherm
Optimization
Malachite Green
Clay

چکیده

جذب مالاشیت گرین از محلول آبی با استفاده از جاذب کم هزینه محلی، خاک رس Ntezi فعال شده با اسید بررسی شده است. جاذب کم هزینه با غلظت های مختلف از اسید سولفوریک، فعال و خواص فیزیکو شیمیایی جاذب تعیین شد. خواص ساختاری با استفاده از XRF و XRD آنالیز شده است. فرایند جذب به صورت تابعی از پارامترهای مختلف فرایند از قبیل دما، مقدار جاذب، زمان تماس، اندازه ذره و سرعت همزن مطالعه گردید. پارامترهای فرایند با استفاده از روش پاسخ سطح (RSM) بهینه شد. اهمیت پارامترهای مختلف فرایندی و اثر ترکیب آنها روی بازده جذب از طریق طراحی ترکیب مرکزی فاکتوریل کامل پایه گذاری شد. مدل سازی تعادل با استفاده از معادلات لانگمویر، فرندلیچ، دوبینی- رادوشکویچ و ایزوترم تمکین آنالیز شد. نتایج آزمایشگاهی از ایزوترم جذب لانگمویر پیروی کرد. سینتیک جذب از معادله شبه درجه دوم با نفوذ خارج ذره ای به عنوان مرحله تعیین کننده سرعت پیروی کرد. این بررسی نشان داد که خاک رس معدنی محلی می تواند اصلاح شود و به عنوان یک جاذب خوب برای حذف ناخالصی ها از آب مورد استفاده قرار گیرد.

doi: *10.5829/idosi.ije.2014.27.06c.03*